

Amphiphiles with different chemical structures and arrangement of hydrophilic and hydrophobic groups have been reported, and their structural features determine the morphological and functional properties of those self-assemblies formed in water.<sup>[15]</sup> The formation of vesicles from mono-alkylphenol derivatives is in theory unexpected because of the conelike shape of the molecules and the high  $pK_a$  value of the OH groups. In fact, alkylresorcinol **3**, which has an alkyl chain as long as that in **1** and **2** but lacks a macrocyclic structure, forms micellelike aggregates under conditions identical to those described here. Aggregates of **3** with diameters less than 16 nm were confirmed by AFM.<sup>[16]</sup> In contrast, owing to the macrocyclic structures of **1** and **2** composed of four alkylresorcinol and alkylpyrogallol moieties, respectively, the amphiphiles have a cylindrical shape, and thus vesicles are the preferred morphology of aggregates formed in water.

The FT-IR spectrum of the dehydrated vesicles of **1** shows the stretching band of the hydrogen-bonded OH groups ( $3500\text{ cm}^{-1}$ ).<sup>[17]</sup> A pair of hydroxyl groups on adjacent benzene rings form a hydrogen bond due to their proximity, which stabilizes the all-axial and all-*cis* configuration, and probably promotes the dissociation of one OH group in the pair at the experimental pH. This also suggests the existence of intermolecular OH...O hydrogen bonds. This phenomenon along with the shape of the amphiphile and hydrogen bonds in **1** and **2** should help stabilize the vesicle structure. To the best of our knowledge this is the first example in which a phenolic surfactant self-assembles to furnish a vesicle.

We have shown that a macrocycle consisting of four phenolic amphiphiles and having a cylindrical molecular shape self-assembles selectively to form a vesicle. The intra- and intermolecular hydrogen bonds between OH groups on **1** and **2** play an essential role in stabilizing the assembled structure. This work, therefore, may open the way for the study of calixarenes in assembled form, in contrast to previous studies dealing mainly with their unimolecular function.

Received: November 24, 1997

Revised version: October 26, 1998 [Z11191IE]

German version: *Angew. Chem.* **1999**, *111*, 565–567

**Keywords:** calixarenes • hydrogen bonds • self-assembly • vesicles

- [1] a) J. H. Fendler, *Membrane Mimetic Chemistry*, Wiley, New York, **1982**; b) T. Kunitake, *Angew. Chem.* **1992**, *104*, 692; *Angew. Chem. Int. Ed. Engl.* **1992**, *31*, 709.
- [2] a) *Liposomes as Drug Carriers: Recent Trends and Progress*, (Ed.: G. Gregoriadis), Wiley, Chichester, **1988**; b) A. Kay, M. Grätzel, *J. Phys. Chem.* **1993**, *97*, 6272.
- [3] Y. Tanaka, Y. Kobuke, M. Sokabe, *Angew. Chem.* **1995**, *107*, 717; *Angew. Chem. Int. Ed. Engl.* **1995**, *34*, 693.
- [4] For the formation of vesicles from macrocyclic amphiphiles see: a) S. Arimoto, T. Nagasaki, S. Shinkai, *J. Chem. Soc. Perkin Trans. 2* **1995**, 679; b) P. Ghosh, T. Khan, P. K. Bharadwaj, *Chem. Commun.* **1996**, 189, and references therein. For the self-assembly of calix[4]resorcinarene in an organic solvent see: c) L. R. MacGillivray, J. L. Atwood, *Nature* **1997**, *389*, 469.
- [5] To remove the organic solvent the aqueous buffer was heated at  $60^\circ\text{C}$ . The spherical particles were also obtained by sonication of the buffer containing macrocyclic amphiphiles. Compound **2** was obtained as colorless crystals and the spectroscopic data ( $^1\text{H}$  and  $^{13}\text{C}$  NMR, IR, and mass spectra) were consistent with the given structure. The

dodecaacetylated derivative of **2** was used to obtain a correct C,H,O analysis because of the extremely high hygroscopicity of unsubstituted **2**.

- [6] Electron micrographs were recorded on JEOL TEM-2000F and TEM-1010 instruments. The freeze-fracture replicas were fabricated with a JEOL JFD-9010 instrument.
- [7] For AFM measurements of vesicles and the determination of their shape, diameter, and thickness, and estimation of the number of membrane layers, see: S. Singh, D. J. Keller, *Biophys. J.* **1991**, *60*, 1401.
- [8] AFM images were recorded on an SPI-3700 instrument from Seiko Instruments Inc. operating in cyclic contact and noncontact modes using a silicon cantilever with force constants of  $20\text{ N m}^{-1}$  and  $3\text{ N m}^{-1}$ , respectively, under atmospheric conditions. These two operating modes provided almost the same images for an identical sample.
- [9] The vesicle solution ( $2.5 \times 10^{-3}\text{ M}$ , 4 mL) containing a fluorescent dye (sodium 8-amino-1,3,6-naphthalenetrisulfonate, 34.2 mg) was separated with Sephadex G-50 ( $1\text{ cm} \times 20\text{ cm}$ ) using the buffer as the eluent. The vesicles were obtained in the 0.36–0.63 mL fraction, whereas the free dye was obtained after elution of 0.9 mL. The vesicle fraction fluoresced at 515 nm when irradiated at 370 nm.
- [10] a) Y. Aoyama, Y. Tanaka, S. Sugahara, *J. Am. Chem. Soc.* **1989**, *111*, 5397; b) Y. Tanaka, Y. Aoyama, *Bull. Chem. Soc. Jpn.* **1990**, *63*, 3343.
- [11] J. Sunamoto, K. Iwamoto, H. Kondo, *Biochem. Biophys. Res. Commun.* **1980**, *94*, 1367.
- [12] J. N. Israelachvili, *Intermolecular and Surface Forces*, 2nd ed., Academic Press, London, **1992**.
- [13] DSC was recorded on a Perkin Elmer Pyris 1 instrument. Measurements were repeated four times for the same sample with a heating cycle of 15 to  $90^\circ\text{C}$ . The reproducibility of the peak top temperature ( $T_c$ ) was  $\pm 0.5^\circ\text{C}$ . After the sample had been cooled to  $-50^\circ\text{C}$  it showed a higher  $T_c$  of  $82.6^\circ\text{C}$ .
- [14] Y. Okahata, R. Ando, T. Kunitake, *Ber. Bunsen-Ges. Phys. Chem.* **1981**, *85*, 789.
- [15] J. N. Israelachvili, D. J. Mitchell, B. W. Ninham, *J. Chem. Soc. Faraday Trans. 1* **1976**, *72*, 1525.
- [16] C. Huang, J. T. Mason, *Proc. Natl. Acad. Sci. USA* **1978**, *75*, 308.
- [17] For IR spectra of the dried vesicles and the contribution of hydrogen bonds towards the stabilization of the vesicle, see: T. Shimizu, M. Kogiso, M. Masuda, *Nature* **1996**, *383*, 487.

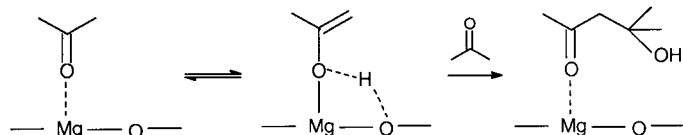
## Adsorption of Acetone onto MgO: Experimental and Theoretical Evidence for the Presence of a Surface Enolate\*\*

Javier F. Sanz,\* Jaime Oviedo, Antonio Márquez,  
José Antonio Odriozola, and Mario Montes

Basic catalysts are widely used in heterogeneous catalytic processes either as supports or active components. Among these processes, aldol condensation of ketones is of out-

- [\*] Prof. Dr. J. F. Sanz, Dr. J. Oviedo, Prof. Dr. A. Márquez  
Departamento de Química Física, Facultad de Química  
Universidad de Sevilla  
E-41012, Sevilla (Spain)  
Fax: (+349) 954-557-174  
E-mail: sanz@cica.es
- Prof. Dr. J. A. Odriozola  
Departamento de Química Inorgánica e Instituto de Ciencias de los  
Materiales de Sevilla  
Universidad de Sevilla-CSIC (Spain)
- Prof. Dr. M. Montes  
Departamento de Química Aplicada, Facultad de Química  
Universidad del País Vasco, San Sebastián (Spain)
- [\*\*] This work was supported by the DGICYT (Spain, project no. PB95-1247) and by the European Commission (contract no. ERBCT1-CT94-0064).

standing industrial interest. For example, aldol addition of acetone gives diacetone alcohol (DAA), which is used as a cellulose solvent and also as an intermediate in the synthesis of methyl isobutyl ketone, an important solvent in the chemical industry. From a mechanistic point of view, aldol additions are base-catalyzed reactions which occur through formation of an enolic species on a basic center of the MgO surface, which then adds to a C=O double bond to yield DAA (Scheme 1).



Scheme 1.

Although the catalytic activity of MgO is lower than other more basic solids, such as heavier alkaline earth oxides<sup>[1]</sup> or aluminum phosphorous oxinitrides catalysts,<sup>[2]</sup> its well-known structure makes it suitable for mechanistic studies.<sup>[3]</sup> In fact, the acetone–MgO system has been the subject of several infrared and temperature-programmed desorption studies,<sup>[4]</sup> and  $^1\text{H}$ – $^2\text{H}$  exchange experiments have also been reported.<sup>[5]</sup> Despite all this work, some aspects of the surface reaction still remain open. In particular, the  $^1\text{H}$ – $^2\text{H}$  exchange studies suggested a slow formation of the C–C bond by reaction of the enolate species with acetone. However, no spectroscopic evidence for the presence of an enol species on the MgO surface has been reported. This could, in principle, be due to poor resolution of the earlier IR spectra, and we were prompted to revisit this system using a much more sophisticated tool based on diffuse reflectance Fourier transform techniques (DRIFT). Such a study was found to be of increased interest when a recent theoretical paper was taken into account.<sup>[6]</sup> The effect of a MgO surface on the keto–enol equilibrium for acetone was shown to significantly decrease the energy difference between the keto and enol tautomers. Such a stabilization of the enol tautomer necessarily involves an increment of its surface concentration, which would account for the catalytic activity of the surface.

With the aim of investigating the presence of an enolic tautomer on the MgO surface, we undertook a DRIFT spectroscopic study of the acetone–MgO system. The most outstanding result is the appearance of a new band at  $1640\text{ cm}^{-1}$  which could be assigned to an adsorbed enolic species. To support this interpretation, theoretical calculations of the vibrational frequencies for acetone and isopropenol chemisorbed on a MgO surface have been performed. These computations were carried out by means of second-order Möller–Plesset *ab initio* Hartree–Fock cluster-embedded calculations.

The DRIFT spectra were recorded with a Nicolet 510P spectrometer equipped with a high-temperature cell with a volume of about  $1.5\text{ cm}^3$  (Spectra-Tech) and ZnSe windows. MgO samples were outgassed *in situ* at  $500^\circ\text{C}$  under a flow of nitrogen. The spectrum of such a sample was taken as the reference for the later enhancement of the contribution of

adsorbed species. Nitrogen gas was bubbled through a saturator which contained acetone at  $25^\circ\text{C}$ ; this stream was then admitted into the DRIFT cell. In Figure 1 b, the spectrum

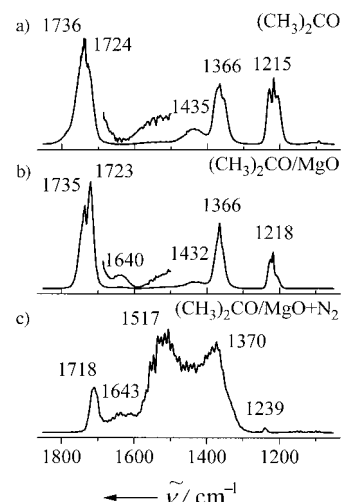


Figure 1. Experimental room-temperature DRIFT spectra. a) Acetone in the gas phase. b) MgO in contact with dry  $\text{N}_2$  and acetone vapor. c) After outgassing in a dry  $\text{N}_2$  flow. Intensities in arbitrary units.

of the adsorbed phase, recorded in a flow of acetone, is reported in the  $800\text{--}2000\text{ cm}^{-1}$  region. For comparative purposes, the spectrum of gas-phase acetone recorded under the same conditions is reported in Figure 1 a. In this case, the intensity of the interferogram was ratioed to the signal which corresponded to an aluminum mirror. When these spectra are compared, they appear quite similar. In the acetone–MgO system, two bands are observed in the CO stretching region ( $1735$  and  $1723\text{ cm}^{-1}$ ), in agreement with high-resolution spectra of ketones. These two peaks are generally explained by a Fermi resonance between the fundamental CO vibration and an overtone. The shift of these frequencies with respect to the gas-phase IR spectrum ( $1739$ ,  $1724\text{ cm}^{-1}$ ) is negligible and within the resolution of the instrument ( $4\text{ cm}^{-1}$ ), which indicates weak physisorption of an electrostatic nature between the acetone molecule and the surface, in agreement with previous theoretical work.<sup>[6]</sup> This band is followed by a small shoulder at  $1640\text{ cm}^{-1}$  which is not present in the gas-phase spectrum of acetone and is clearly appreciable in the overlaid spectrum obtained after amplification by a factor of ten. The intense bands in the  $1437\text{--}1365\text{ cm}^{-1}$  region correspond to symmetric and asymmetric bending vibrations of methyl groups, while the  $1207\text{--}1225\text{ cm}^{-1}$  absorption bands are commonly assigned to C–C stretching vibrations. In summary, both spectra are similar, with the exception of the  $1640\text{ cm}^{-1}$  band, whose presence suggests the formation of a new surface species. It should be noted that this band is observed in a relatively wide range of experimental conditions, from room temperature up to  $140^\circ\text{C}$ . At higher temperatures, new signals which correspond to addition products are observed.

A further point was to determine whether this band is due to a species directly adsorbed on the surface or if it is due to a species present in a possible multilayer. Therefore, acetone

was flushed out of the cell by a dry  $N_2$  flow. Under these conditions, it is expected that only strongly adsorbed species will remain. As shown in Figure 1c, the spectrum is dominated by the strong absorption bands of carboxylate-like species<sup>[7]</sup> which arise from the well-known oxidation reaction of acetone on metal oxide surfaces;<sup>[8–10]</sup> the  $1640\text{ cm}^{-1}$  band is still present, however. This band cannot be assigned to the water-bending mode since, firstly, the spectra are displayed with MgO under the same conditions as the reference. Secondly, inspection of the OH region of the spectrum shows that the band associated to hydrogen-bridged OH groups has a very low intensity and it is known that the intensity of the water-bending vibration is even less intense. Moreover, this band could be correlated with those observed in the FT-IR spectra of acetone adsorbed on vanadia-titania ( $1565\text{ cm}^{-1}$ ) and  $Fe_2O_3$  ( $1540\text{ cm}^{-1}$ ) surfaces,<sup>[8, 11]</sup> and which have been assigned to an enolate species because of their similarity to the band at  $1582\text{ cm}^{-1}$  observed in a solution of the sodium salt of malonaldehyde in DMSO.<sup>[12]</sup>

To attempt a more reliable assignment of this band, *ab initio* embedded-cluster calculations of the vibrational spectrum for both acetone and isopropanol adsorbed on a MgO (100) surface were undertaken. To model the surface, a  $[MgO_5]^{8-}$  cluster embedded in an array of model potentials and point charges was chosen as described in reference [6]. For the  $Mg^{2+}$  cation, the basis set proposed by Huzinaga was used,<sup>[13]</sup> enlarged with two s primitive functions to represent the 3s orbital; the contraction was (9s4p)/[4s2p]. For surface oxygen atoms, the basis set optimized for  $O^-$  was chosen, with the (9s5p)/[4s3p] contraction.<sup>[14]</sup> The standard DZP basis set was used for the carbon, oxygen, and hydrogen atoms of the adsorbate. In the calculations, surface ions were fixed at their ideal crystallographic positions ( $d(Mg-O) = 2.105\text{ Å}$ <sup>[15]</sup>), while the adsorbed acetone or isopropanol geometries were optimized at the MP2 level of theory.<sup>[16]</sup> The equilibrium geometries are reported in Figure 2. As can be seen, acetone

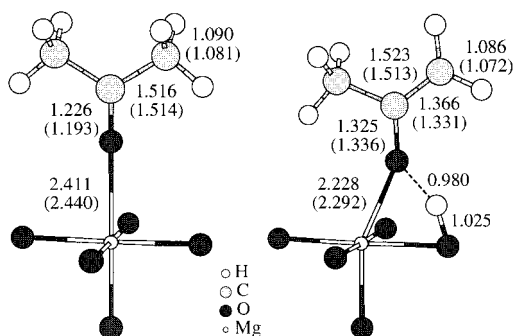


Figure 2. Selected optimized structural parameters for acetone (left) and isopropanol (right) adsorbed on a MgO (100) surface obtained from *ab initio* MP2 embedded-cluster calculations. Values in parentheses are those obtained at the Hartree–Fock level.

adsorbs with the carbonyl group perpendicular to the surface through interaction between a  $Mg^{2+}$  cation and the oxygen atom, with local  $C_{2v}$  symmetry. Isopropanol dissociates to give the corresponding enolate and a proton bound to a surface oxygen atom. It should be noted that at the HF level (values in parentheses), the preferred form is the enol instead of the

enolate, as previously mentioned,<sup>[6]</sup> where the enolate was only found when the surface was allowed to relax.

Vibrational frequencies and intensities of infrared bands were then computed, and the results are summarized in Figure 3. The spectrum for the acetone–MgO system is

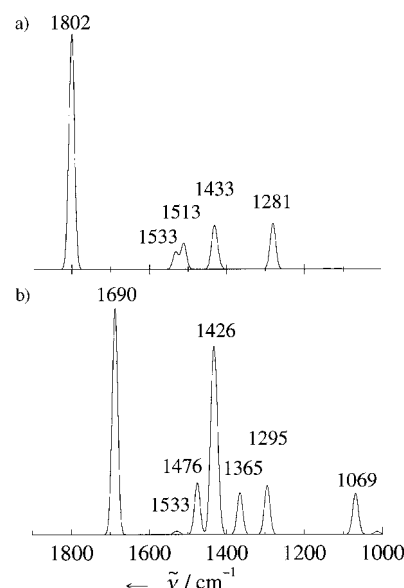


Figure 3. Theoretical IR spectra for a) acetone and b) enolate adsorbed on MgO obtained from *ab initio* MP2 embedded-cluster calculations. Intensities in arbitrary units.

reported in Figure 3a, and excellent agreement is found with the experimental spectrum, both in the shape and position of the bands. The theoretical frequencies appear to be somewhat higher, and the differences ( $50\text{--}70\text{ cm}^{-1}$ ) agree with the shifts known for the harmonic approximation. Figure 3b shows the IR spectrum of the enolate–MgO system. The most outstanding feature of this spectrum is the band computed at  $1690\text{ cm}^{-1}$  which, after the analysis of its associated normal coordinate, is unambiguously assigned to the asymmetric stretching vibration of the C–C–O group. The second most intense peak appears at  $1426\text{ cm}^{-1}$  and corresponds to the symmetric stretching vibration mixed with some methyl bending, and, although its intensity is considerable, it would be buried by the bands of acetone and acetate present in this region of the experimental spectra. This frequency agrees with those observed at  $1380\text{ cm}^{-1}$  in the acetone/vanadia-titania spectrum<sup>[8]</sup> and  $1374\text{ cm}^{-1}$  in the malonaldehyde sodium salt spectra.<sup>[12]</sup>

In summary, the present work shows that acetone adsorption on MgO gives rise to a band at  $1640\text{ cm}^{-1}$  in the DRIFT spectrum that, based on a careful theoretical analysis, is assigned to a surface enolate species. This assignment also confirms the proposed origin of the bands observed in the FT-IR spectra of acetone adsorbed on titanium and iron oxides at  $1565$  and  $1540\text{ cm}^{-1}$ . The frequency shift of these bands with respect to the one reported here can be easily understood because, according to our models, the interaction between both acetone and enolate with the surface occurs through coordination of a surface metal center and the oxygen of the

adsorbed molecule. Because of the stronger Lewis character of  $\text{Ti}^{\text{IV}}$  and  $\text{Fe}^{\text{III}}$  centers, a larger adsorbate-surface interaction and, consequently, a weakening of the C–O and C–C–O bonds can be expected.<sup>[17]</sup> Finally, the existence of such an enolate species seems to confirm that the acetone surface condensation reaction occurs through a standard aldol mechanism.

Received: July 1, 1998

Revised version: November 16, 1998 [Z12080IE]

German version: *Angew. Chem.* **1999**, *111*, 567–570

**Keywords:** ab initio calculations • enols • heterogeneous catalysis • IR spectroscopy • surface chemistry

- [1] G. Zhang, H. Hattori, K. Tanabe, *Appl. Catal.* **1988**, *36*, 189.
- [2] a) P. Grange, P. Bastians, R. Conacec, R. Marchand, Y. Laurent, L. Gandia, M. Montes, J. F. Sanz, J. A. Odriozola, *Stud. Surf. Sci. Catal.* **1995**, *91*, 381; b) R. Marchand, R. Conacec, Y. Laurent, P. Bastians, P. Grange, L. Gandia, M. Montes, J. F. Sanz, J. A. Odriozola (Université de Rennes 1, Université Catholique de Louvain, Universidad del Paris Vasco, Universidad de Sevilla, Cernix), FR-B 9401081 **1994**.
- [3] When MgO is used as the catalyst in a fixed-bed reactor at 1 atm and 200 °C, acetone condensation takes place with a conversion of around 4 %, with 85 % selectivity to mesityl oxide (4-methyl-3-penten-2-one) and 15 % to isomesityl oxide.
- [4] a) J. A. Lercher, H. Noller, G. Ritter, *J. Chem. Soc. Faraday Trans. 1* **1981**, *77*, 621; b) H. Miyata, Y. Toda, Y. Kubokawa, *J. Catal.* **1974**, *32*, 155.
- [5] G. Zhang, H. Hattori, K. Tanabe, *Appl. Catal.* **1988**, *36*, 183.
- [6] J. Oviedo, J. F. Sanz, *Surf. Sci.* **1998**, *397*, 23.
- [7] C. Xu, B. E. Koel, *J. Chem. Phys.* **1995**, *102*, 8158.
- [8] V. Sánchez Escribano, G. Busca, V. Lorenzelli, *J. Phys. Chem.* **1990**, *94*, 8939.
- [9] H. Knözinger, H. Kitenbrink, H. D. Müller, W. Schulz, *Proc. 6th ICC* (London, UK) **1976**, 183.
- [10] E. W. Thornton, P. G. Harrison, *J. Chem. Soc. Faraday Trans. 1* **1975**, *71*, 2468.
- [11] G. Busca, V. Lorenzelli, *J. Chem. Soc. Faraday Trans. 1* **1982**, *78*, 2911.
- [12] W. O. George, V. G. Mansell, *Spectrochim. Acta* **1968**, *24*, 145.
- [13] S. Huzinaga, *Gaussian Basis Sets for Molecular Calculations*, Physical Science Data 16, Elsevier, Amsterdam, **1984**.
- [14] J. Q. Broughton, P. S. Bagus, *Phys. Rev. B* **1984**, *30*, 4761; J. Q. Broughton, P. S. Bagus, *Phys. Rev. B* **1987**, *36*, 2813.
- [15] R. W. Wyckoff, *Crystal Structures*, Wiley, New York, **1963**.
- [16] M. Dupuis, S. Chin, A. Márquez in *Relativistic and Electron Correlation Effects in Molecules and Clusters* (Ed.: G. L. Malli), NATO ASI Series, Plenum Press, New York, **1992**.
- [17] J. Oviedo, C. J. Calzado, M. A. San Miguel, A. Márquez, J. F. Sanz, *J. Mol. Struct. (Theochem.)* **1997**, *390*, 177.

## Chemo-Enzymatic Synthesis of Fluorescent Rab 7 Proteins: Tools to Study Vesicular Trafficking in Cells\*\*

David J. Owen, Kirill Alexandrov, Elena Rostkova, Axel J. Scheidig, Roger S. Goody,\* and Herbert Waldmann\*

Proteins that are S-farnesylated and S-geranylgeranylated at C-terminal cysteine residues play critical roles in cell processes such as signal transduction and intracellular trafficking.<sup>[1–3]</sup> Although our understanding of the biological consequences of protein prenylation has increased significantly over the last few years, there is still relatively little known about the molecular details that govern its functional role, for instance in vesicular trafficking. A particularly relevant example is the role of the Rab proteins in intracellular membrane trafficking. The Rab proteins are a group of small G-proteins that associate with specific membrane components. They are believed to control the events of docking and fusion of intracellular vesicles.<sup>[4]</sup> Rab proteins are subjected to geranylgeranylation through a process that involves Rab geranylgeranyltransferase (RabGGTase) and an accessory protein termed a Rab escort protein (REP). Thus, in order to undergo prenylation, a newly synthesized Rab protein must bind and form a stable complex with REP, which only then (in contrast to other known prenyltransferases) is recognized by RabGGTase.<sup>[5, 6]</sup> Upon prenylation the Rab protein remains bound to REP and accompanies it to the corresponding membrane.<sup>[7]</sup> Subsequent REP-mediated membrane insertion of prenylated Rab proteins is believed to proceed through a putative membrane receptor. The free REP protein is then released and can support another round of Rab prenylation.

Unfortunately, very little is known about the molecular details of this general scenario. Major questions such as whether the lipid groups participate in protein–protein recognition, or the exact mechanism by which the lipidated Rab/REP complex is directed to specific intracellular compartments remain unanswered. Furthermore, despite a number of related reports, the exact affinities of RabGGTase for its lipid substrate are unknown, and the reaction mechanism of the prenylation reaction is also unelucidated. Specific fluorescent probes should enable the dissection of the reaction mechanism through the use of fluorescent spectroscopy. Such probes would allow real-time imaging of the

[\*] Prof. Dr. R. S. Goody, Dr. K. Alexandrov, M.Sc. E. Rostkova, Dr. A. S. Scheidig  
Abteilung Physikalische Biochemie  
Max-Planck-Institut für Molekulare Physiologie  
Rheinlanddamm 201, D-44139 Dortmund (Germany)  
Prof. Dr. H. Waldmann, Dr. D. J. Owen  
Institut für Organische Chemie der Universität  
Richard-Willstätter-Allee 2, D-76128 Karlsruhe (Germany)  
Fax: (+49) 721-608-4825  
E-mail: waldmann@ochhades.chemie.uni-karlsruhe.de

[\*\*] This research was supported by the Deutsche Forschungsgemeinschaft and the Fonds der Chemischen Industrie. D.J.O. gratefully acknowledges financial support from the Alexander von Humboldt Foundation in the form of a postdoctoral fellowship.